

## Limitations on 2D Super-cavitating Hydrofoil Performance

B.W. Pearce and P.A. Brandner

National Centre for Maritime Engineering and Hydrodynamics  
 Australian Maritime College, Launceston, Tasmania, 7250, AUSTRALIA

### Abstract

Classical super-cavitating hydrofoil performance predictions have been based on linearised potential theory for zero cavitation number. More rationalised predictions of super-cavitating hydrofoil performance have been evaluated using a non-linear boundary element formulation. Comparisons are made between flat-plate, circular-arc, and NACA 4-digit camber line wetted surface profiles. Limitations of super-cavitating foil performance are defined in terms of minimum cavity length to avoid instability and the minimum cavity clearance from the hydrofoil wetted surface. The dependence of these limitations on hydrofoil wetted surface profile, incidence and cavitation number are derived.

### Introduction

As the flow speed increases over a hydrofoil section a cavity may form where the local pressure drops below the water vapour pressure. If the cavity closes on the foil surface this is termed a partial cavity, which are often unsteady in nature [11,20], and loss of performance, surface erosion and noise generation can result [3,5,6]. If the cavitation bubble develops to the extent where the cavity closure moves downstream into the wake then it is described as a super-cavity. Although the foil may now no longer be subject to surface erosion, if the cavity closure is just downstream of the foil trailing edge the re-entrant jet may impinge on the foil resulting in buffeting and foil vibration. At a cavity length of 2 foil chords or greater the closure region is typically moved sufficiently downstream that unsteady effects are no longer felt [3,32].

Optimum sub-cavitating (fully wetted) foil sections have an upper speed limit of about 45 knots [6]. For stable operation at higher speeds, where cavitation cannot be avoided, special super-cavitating foil sections were developed which operate with the suction side of the foil completely un-wetted [15,16,31]. This is achieved with the super-cavity forming off sharp leading and trailing edges, as shown in Figure 1. Interest in the use of these super-cavitating hydrofoil sections was directed to high-speed hydrofoil borne craft, super-cavitating propellers and seaplane hydro-skis [6,16,30].

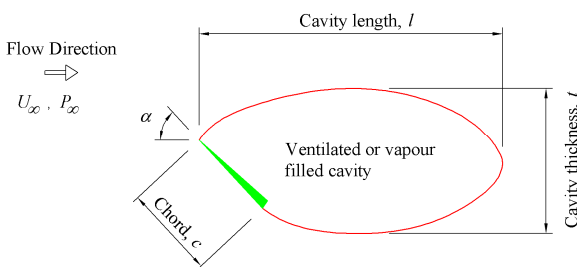


Figure 1. Super-cavitating hydrofoil

The initial development of these sections was based on classical analytical hydrodynamic methods (free-streamline flows) [21,25]. This began in the mid 1950's with the use of linearised theory for the zero cavitation number (infinite cavity length) case [13,31,33]. Extensive experimental programs involving hydrofoils [7,9,10,22,28] accompanied the development of the analytical theory running through to the 1960's. A summary of the progress of this development up till 1968 highlighting the shortcomings of the theory, particularly with respect to the accurate prediction of flutter, is given by Hsu [14]. Since the work published by Conolly [6] in 1975 little further interest in the development of high-speed hydrofoil borne craft has been reported. Work on the design of super-cavitating propellers continued [29] with the enhancement of boundary element methods [17] to incorporate the modelling of super-cavitating flows by the 1990's [18,19,23,26]. During this period all efforts in 2D super-cavitating foil section development were for application to super-cavitating propellers and not foil borne craft.

This present study involves a preliminary design investigation of 2D super-cavitating hydrofoil performance. It is motivated by the requirement for a suitable foil section for the novel application of an ultra-high speed sailing yacht. A boundary element method has been chosen for this analysis as it offers, particularly in the case of complex section shapes, a computationally efficient solution [4].

### Numerical Method

A numerical code incorporating a low-order, non-linear, boundary element formulation has been developed by the authors using the methods of Kinnas & Fine [19] and Lee et al. [23]. The method is potential based employing both normal doublets and sources distributed on the foil and cavity surfaces. The cavity shape and surface velocity are unknown for a fixed cavity length and introduce non-linearity to the problem necessitating an iterative solution.

In the present context the cavitation number is defined as a cavity under-pressure coefficient:

$$\sigma_c = \frac{p_\infty - p_c}{\frac{1}{2} \rho U_\infty^2} \quad (1)$$

where  $p_\infty$  is the static pressure at the foil submergence,  $p_c$  the cavity pressure and the denominator is the freestream dynamic pressure with  $\rho$ , the fluid density and  $U_\infty$ , the freestream velocity. The cavity pressure may be either the vapour pressure of the water for a naturally occurring or "vapour super-cavity" or some higher value due to the admission of a non-condensable gas (usually air) into a "ventilated super-cavity". It is the value of  $\sigma_c$  which determines the cavity characteristics and the hydrodynamic forces that result, regardless of how  $\sigma_c$  is obtained.

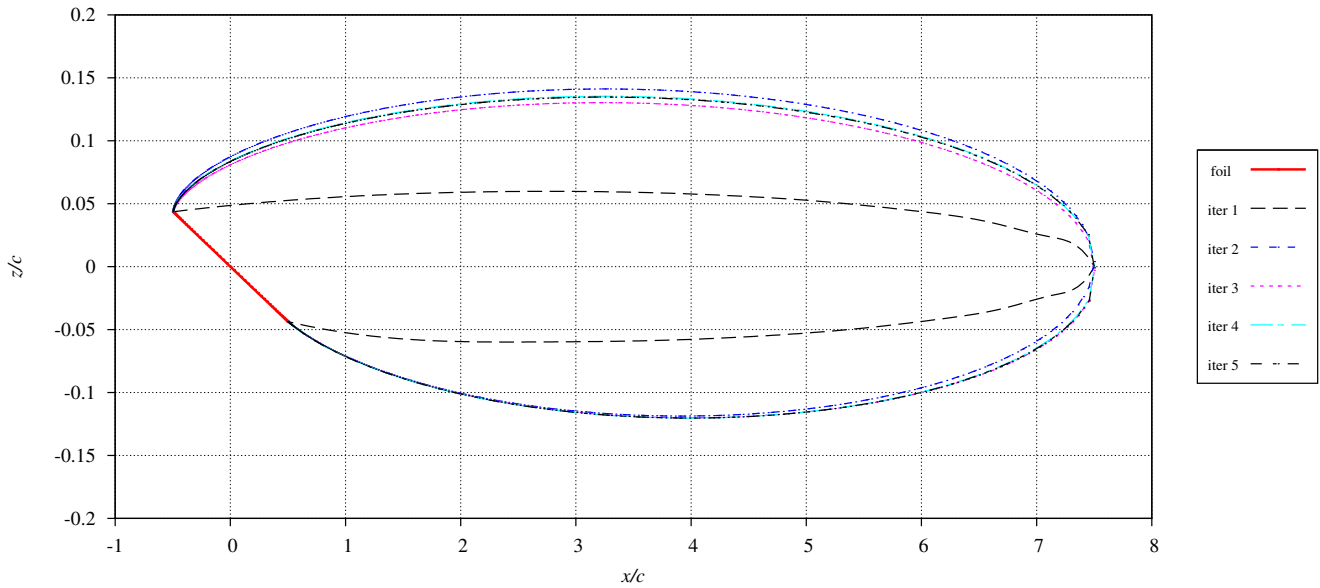


Figure 2. Iterations in dimensionless cavity shape for a flat-plate supercavitating hydrofoil with  $\alpha = 5^\circ$  and  $\sigma_c = 0.66$

Within the numerical solution, the final cavity shape is derived by normal convection from an initial arbitrary position until the dual-conditions of flow tangency (kinematic boundary condition) and constant pressure (dynamic boundary condition) along the cavity surfaces are simultaneously satisfied. The method is seen to converge well after only a small number of iterations (typically within 3 or 4). This behaviour is shown in Figure 2 for the cavity shape and in Figure 3 for both the lift coefficient,  $C_L$ , and cavitation number,  $\sigma_c$ . The foil and cavity surfaces are shown plotted with coordinates non-dimensionalised on the foil chord length,  $c$ .

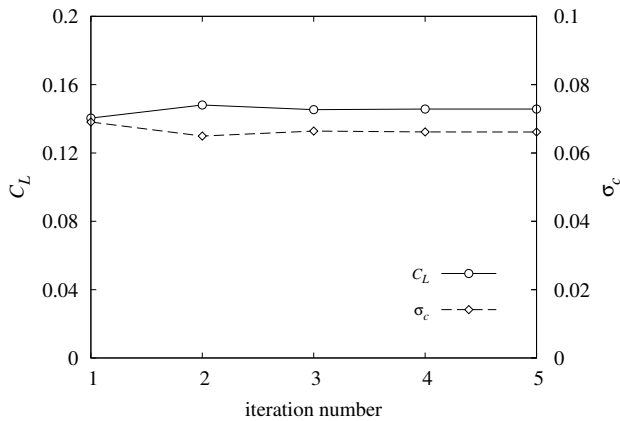


Figure 3. Convergence of  $C_L$  and  $\sigma_c$  with iteration number for a flat-plate supercavitating hydrofoil with  $\alpha = 5^\circ$  and  $\sigma_c = 0.66$

The discretisation of the foil and cavity surfaces involves consideration of several issues. Numerical differentiation of the surface potential is required to calculate surface velocity and so element lengths need to vary smoothly to minimise error. Elements also need to be finely graded in regions of high pressure gradient and surface curvature. For computational efficiency a cosine discretisation has been implemented to obtain the small element lengths required at the ends of the surfaces. Figure 4 shows a typical example of the discretised surfaces. To maintain smooth variation of element lengths across the foil/cavity interfaces element numbers on the cavity surface are adjusted with cavity length. In the same way if the number of

elements on the foil is varied the number of cavity elements is varied to suit. Parameter convergence with increasing number of elements, for a constant  $\alpha$  and  $\sigma_c$ , are shown in Figure 5. A converged solution in this case is achieved by 100 to 150 foil elements.

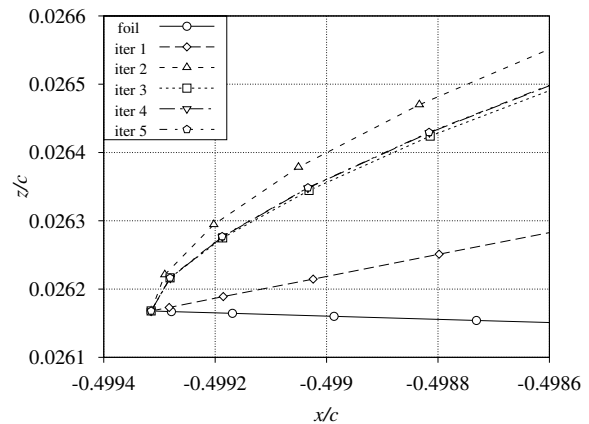


Figure 4. Surface discretisation in the vicinity of the leading edge, for a n4cl\_1\_70 profile with  $\alpha = 3^\circ$  and  $\sigma_c = 0.05$ . Number of elements on foil wetted surface = 260 and number of elements on cavity surfaces = 1100

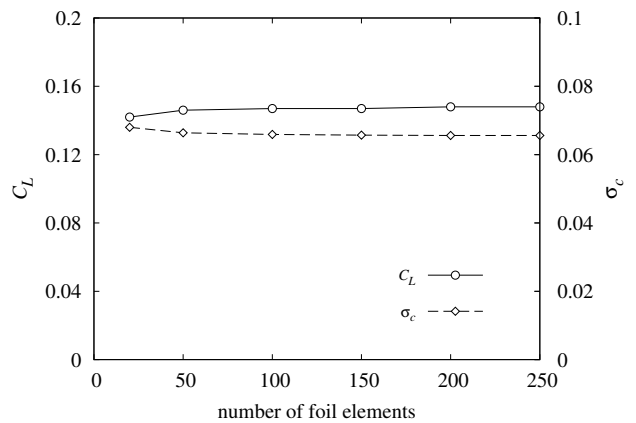


Figure 5. Convergence with number of elements for a flat-plate supercavitating hydrofoil with  $\alpha = 5^\circ$  and  $\sigma_c = 0.66$

For the present analysis the foil wetted surface has been discretised with 260 elements. The greater number of elements required in this case to obtain a stable solution of cavity shape for the thin cavities present at low incidence. This numerical instability is due to the spacing of the foil and upper cavity surfaces relative to the length of the elements in the vicinity. For a stable solution the surfaces need to have a minimum separation of the order of the local element length.

Also of concern is the discretisation in the vicinity of the cavity closure region. The implementation used for this analysis did not include an explicit closure model to account for the deceleration of the cavity surface velocity back to free stream value. If the elements in the closure region are too small a re-entrant jet type structure forms as the cavity surface is adjusted with successive iterations. These solutions are numerically unstable and do not converge. Increasing the element size in the closure region by using a half-cosine discretisation on each cavity surface removes this behaviour and results in a stable solution. By not properly modelling the physics of the closure region some error will likely be inherent in the solution. It is assumed that with the closure far away from the foil it will have a negligible effect on the local flow geometry about the foil and hence the forces produced. This is a reasonable assumption except possibly for the shorter cavities as the comparison with experiment and theory shows (Figure 8). A cavity termination model [19] which uses a transition length over which the velocity is continuously varied between the constant value on the cavity surface down to the freestream value was implemented and assessed. It however made little difference to the results obtained and in any case is an artifice as the re-entrant jet cavity closure is an inherently unsteady structure dominated by viscous forces and so cannot be accounted for within a steady potential flow method. The results obtained show that de-resolving of the re-entrant jet behaviour gives adequate flow modelling for super-cavities of practical length.

To assess the effect of varying geometry on performance three classes of hydrofoil wetted profiles were analysed. The flat-plate profile gives the effect due solely to the variation of incidence,  $\alpha$ . Effect of camber was assessed with a circular-arc profile with an increase in camber generated by a larger subtended angle,  $\gamma$ . Profiles with  $\gamma = 2^\circ, 2.29^\circ, 4^\circ$  &  $8^\circ$  (designated as ca2, ca2.29, ca4 & ca8) were analysed (see Figure 6). The third effect examined was that of moving the location of maximum camber away from the mid-chord position. This was achieved with the use of the NACA 4-digit mean camber line [1] which is a composite of two sections. The first section is that forward of the maximum ordinate and is defined by:

$$z = \frac{m}{p^2} (2px - x^2) \quad (2)$$

with the section aft of the maximum ordinate defined by:

$$z = \frac{m}{(1-p)^2} (1-2p+2px-x^2) \quad (3)$$

Where  $m$  is the maximum ordinate of mean line expressed as a fraction of chord and  $p$  is the chordwise position of maximum ordinate. A NACA 4-digit mean camber line profile with  $m = 1\%$  and  $p = 70\%$  is designated as n4cl\_1\_70. Two of these profiles together with a circular-arc profile ( $\gamma = 2.29^\circ$ ) of equivalent camber are shown in Figure 7.

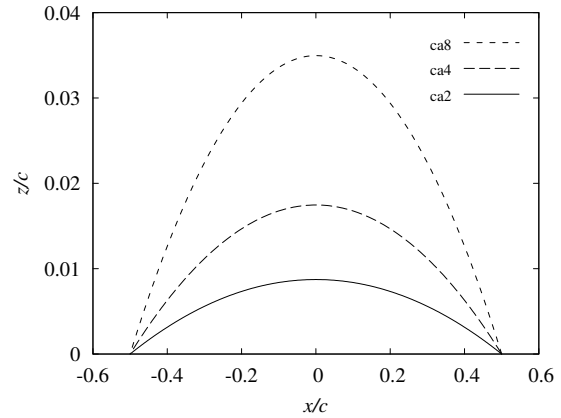


Figure 6. Comparison of circular-arc profiles with  $\gamma = 2^\circ, 4^\circ$  &  $8^\circ$

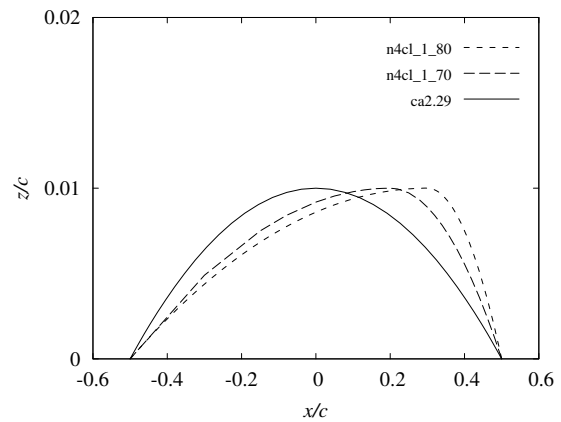


Figure 7. Comparison of NACA 4-digit mean camber and ca2.29 profiles

## Results

The results given by the present method compare well with those from experiment [28] and the exact theory developed by Wu [33] as shown in Figure 8.

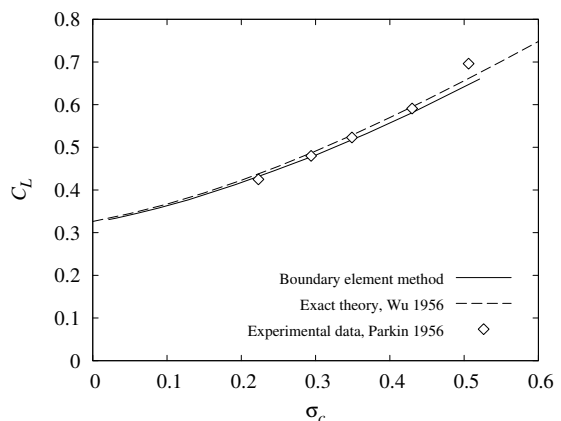


Figure 8. Comparison of boundary element method results with experimental data from Parkin [28] and Wu's exact theory [33] for a flat-plate super-cavitating hydrofoil with  $\alpha = 15^\circ$

The outputs from the boundary element method include the hydrodynamic force coefficients –  $C_L, C_D, C_M$ , the pressure distribution over the foil surfaces and the cavity surface geometry. The force components and moment (about the leading edge) are non-dimensionalised by dividing by the dynamic pressure (as used in Equation 1) and the foil chord length.

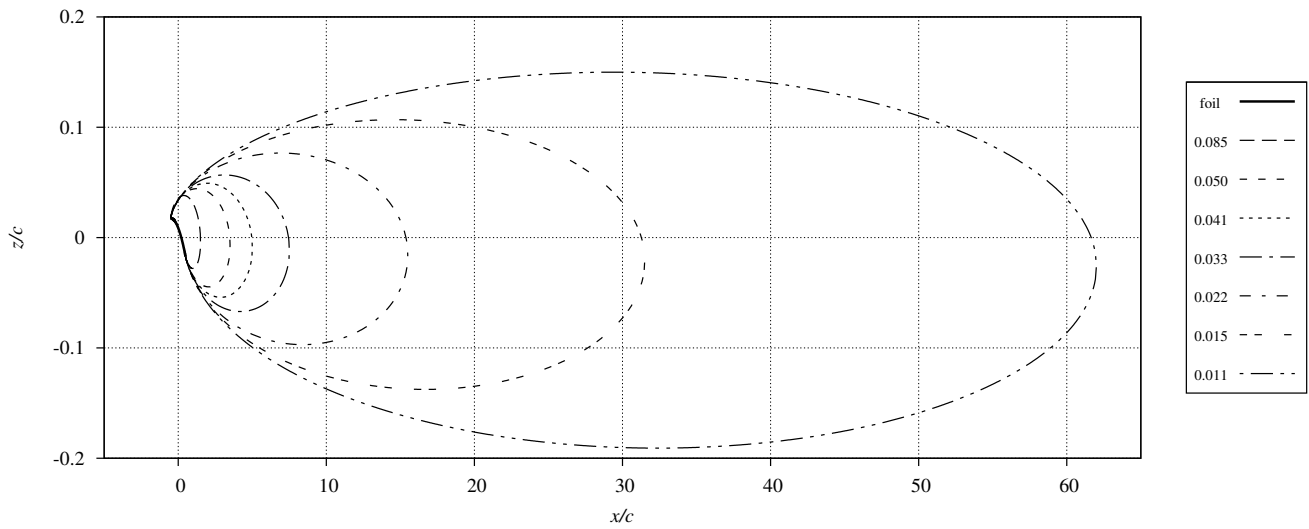


Figure 11. Variation in cavity geometry with reducing  $\sigma_c$  for the ca2 profile with  $\alpha = 2^\circ$

The results show that  $C_L$  increases with camber and with increasing ordinate of maximum camber position (Figure 9). For foil efficiency or lift to drag ratio,  $L/D$ , there is also an increase with camber but this trend is reversed with the change in location of maximum camber, as indicated in Figure 10. Also shown in Figure 10, is that  $L/D$  is only mildly dependent on  $\sigma_c$ . The left hand end of each of the curves in these figures corresponds to the minimum cavity length criteria of 2 chord lengths. The use of the composite parameter  $\sigma_c/2\alpha$  stems from linearized theory. It accounts for the equivalent effect that either a decrease in cavitation number or an increase in incidence has on cavity length [12].

For a fixed incidence the behaviour of the cavity with decreasing  $\sigma_c$  is manifested by an increase in cavity thickness and length, as typified by the circular-arc example shown in Figure 11. The behaviour near the leading edge however does not follow this global pattern. With a reduction of  $\sigma_c$ , the cavity thickness over the forward part of the foil reduces whilst then increasing over the rear section as shown in Figure 12.

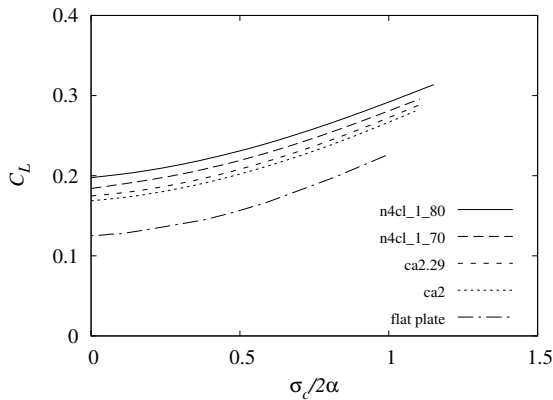


Figure 9. Variation of  $C_L$  with  $\sigma_c/2\alpha$  for various profiles at  $\alpha = 5^\circ$

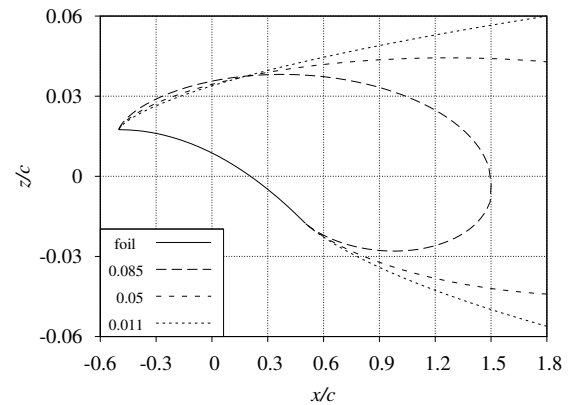


Figure 12a. Change in upper cavity surface shape with variation in  $\sigma_c$  for the ca2 profile at  $\alpha = 2^\circ$

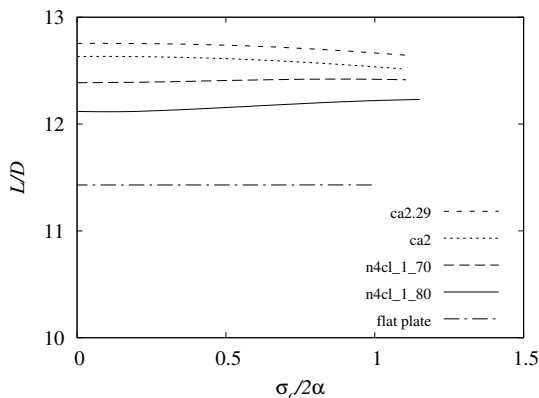


Figure 10. Variation of  $L/D$  with  $\sigma_c/2\alpha$  for various profiles at  $\alpha = 5^\circ$

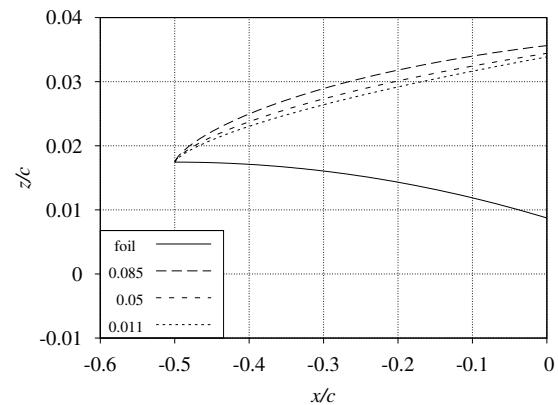


Figure 12b. Change in upper cavity surface shape with variation in  $\sigma_c$  over the forward section of foil for the ca2 profile with  $\alpha = 2^\circ$

Hydrofoil structural requirements dictate the minimum clearance required between upper cavity surface and foil upper surface.

The decrease in cavity thickness in the neighbourhood of leading edge due to reduction of  $\sigma_c$ , as depicted in Figure 12, places a limit on foil maximum thickness before wetting occurs. A similar limitation exists due to reduction of  $\alpha$  (see Figure 13).

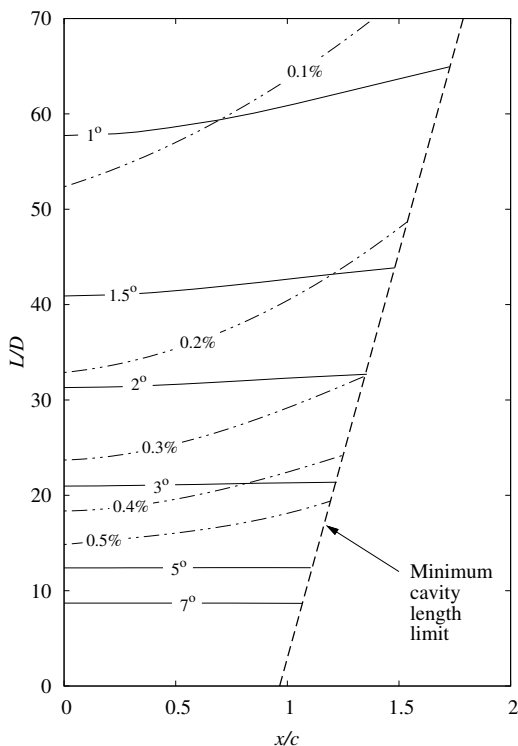


Figure 13. Variation of  $L/D$  with  $\sigma_c/2\alpha$  for the n4cl\_1\_70 profile, solid lines are curves of constant  $\alpha$  with the right hand end of each being the minimum cavity length limit (MCL), dashed lines are curves of constant cavity thickness at 2%  $c$

In comparing the different profiles considering a minimum cavity thickness criterion, the NACA 4-digit camber line profile now performs better than the circular-arc (Figure 14). This is in contrast to the previous comparison at fixed  $\alpha$  (Figure 10). The linear variation of cavity thickness with  $\alpha$  at a constant  $\sigma_c$  is shown in Figure 15. These curves indicate the incidence sensitivity of the profile, from which a tolerance can be derived, for a given foil thickness at a fixed speed and depth of submergence (i.e. at a particular cavitation number).

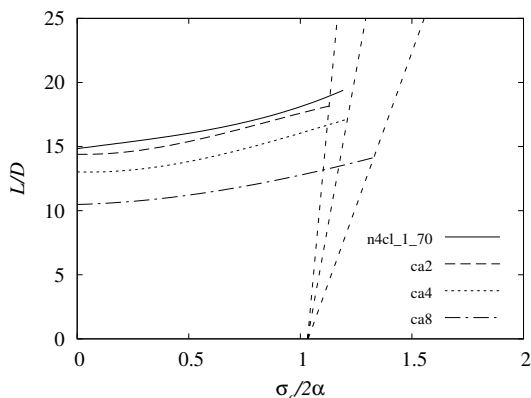


Figure 14. Variation of  $L/D$  with  $\sigma_c/2\alpha$  for various profiles, solid lines are curves of constant cavity thickness - 0.5%  $c$  at 2%  $c$ , dashed lines at the right end of curves are the minimum cavity length limits (MCL) for the circular-arc profiles

## Discussion

From these results an optimum super-cavitating foil is obtained with a profile having a small amount of camber, located aft of the mid-chord position, and operating at the smallest incidence for which a stable cavity will form. If a foil with a thickness of 0.5%  $c$  at 2%  $c$  [3, p16] is chosen as typical of that determined by structural requirements it can be seen from Figure 13 that an  $L/D$  of around 15 is achievable. Testing of this section and a thinner section was reported by Auslaender [3] but with the later found to suffer leading edge flutter. From these results the practicality of the higher  $L/D$  values of over 30 reported by Mishima and Kinnas [26] is questionable. These results also included a viscous drag component by assuming a uniform friction coefficient over the wetted part of the foil. In this analysis Mishima and Kinnas used an acceptable length of cavity appreciably less than the two chords necessary for a stable super-cavity. A minimum cavity thickness criterion was included but the value used was not given. From Figure 13, the trend of increasing  $L/D$  with both reducing cavity thickness and increasing cavitation number (reduction in cavity length) can be seen. The higher  $L/D$  values cited by Mishima and Kinnas can be attributed to the acceptance in their optimisation of unrealistically short and/or thin cavities.

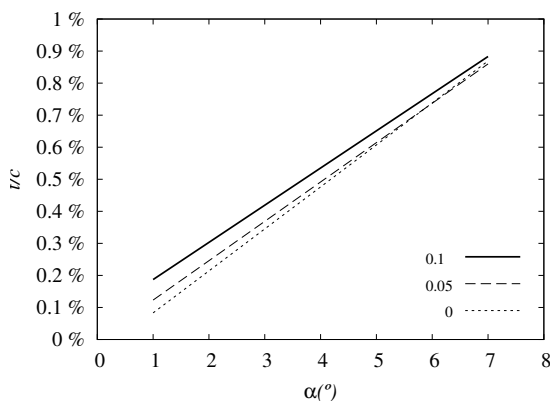


Figure 15. Cavity thickness at 2%  $c$  as a function of  $\alpha$  for the n4cl\_1\_70 profile. The lines are curves of constant  $\sigma_c$

Influences affecting hydrofoil performance that have not been included in the present analysis include the effects of (1) the addition of the viscous drag on the wetted surface of the foil, (2) surface tension and (3) the proximity of the free surface to the hydrofoil. Surface tension has an influence due to the locally high curvature at the foil leading edge, i.e. the cavity detachment point. An analytical investigation by Oba [27] into the effect of surface tension found it to be significant for  $\alpha$  less than  $5^\circ$ . The results indicated a reduction of lift, drag, moment and cavity thickness and the effect was equated to an incidence reduction  $\Delta\alpha$ , proportional to the surface tension of the fluid. To compensate for the effect of surface tension this  $\Delta\alpha$  would need to be added to the incidence of the hydrofoil. The effect of free surface proximity on cavity shape is well covered in the literature with an example of experimental measurements by Altman [2] and numerical investigation by Doctors [8] showing the cavity thickness increasing with decrease of foil submergence.

## Conclusions

For practical operation of a lifting surface the conditions under which the forces and moments are being produced need to remain stable. To ensure a continuous stable cavity for a super-cavitating hydrofoil it must be both of sufficient length and

maintain sufficient thickness so that the upper hydrofoil surface remains un-wetted. To achieve this, allowances need to be added on to the minimum cavity thickness required by the hydrofoil dimensions to account for the effect of surface tension, depth of submergence, incidence tolerance required and any speed variation. These factors will for the most part lead to the operation of the hydrofoil at a greater than optimum incidence, resulting in a reduction in the  $L/D$  achieved. As a starting point an  $L/D$  of around 15, rather than 30 [26], is the optimum achievable for a super-cavitating foil of the section profile types analysed.

## References

- [1] Abbott, I.H. & von Doenhoff, A.E., *Theory of Wing Sections*, Dover Publications Inc., New York, 1959.
- [2] Altmann, R.J., *Measurement of cavity shapes above ventilated hydrofoils*, Hydronautics Inc, Laurel, Md, Technical Report 457-1, 1965.
- [3] Auslaender, J., *Low drag supercavitating hydrofoil sections*, Hydronautics Inc, Laurel, Md, Technical Report 001-7, 1962.
- [4] Brennen, C.E., *Cavitation and Bubble Dynamics*, Oxford University Press, 1995.
- [5] Breslin, J.P. & Andersen, P., *Hydrodynamics of Ship Propellers*, Cambridge, Cambridge University Press, 1994.
- [6] Conolly, A.C., Prospects for very-high-speed hydrofoils, *Marine Technology*, **12**(4), 1975, 367-377.
- [7] Christopher, K.W. & Johnson, V.E., Jr., *Experimental investigation of two low-drag supercavitating hydrofoils at speeds up to 200 feet per second*, NASA TN D-436, 1960.
- [8] Doctors, L.J., Effects of a finite Froude number on a supercavitating hydrofoil, *Journal of Ship Research*, **30**(1), 1986, 1-11.
- [9] Dobay, G.F., *Influence of scale ratio, aspect ratio, and planform on the performance of supercavitating hydrofoils*, NSRDC Report No. 2390, 1967.
- [10] Ficken, N.L. & Dobay, G.F., *Experimental determination of the forces on supercavitating hydrofoils with internal ventilation*, DTMB Report No. 1676, Jan. 1963.
- [11] Franc, J.-P., Partial cavity instabilities and re-entrant jet, in *Fourth International Symposium on Cavitation: CAV2001*, editors C.E. Brennen, R.E.A. Arndt and S.L. Ceccio, California Institute of Technology, 2001.
- [12] Franc, J.-P. & Michel, J.-M., *Fundamentals of Cavitation*, Kluwer Academic Publishers, 2004.
- [13] Geurst, J.A., Linearized theory for fully cavitating hydrofoils, *International Shipbuilding Progress*, **7**(65), 1960, 17-27.
- [14] Hsu, Y.K., A brief review of supercavitating hydrofoils, *Journal of Hydronautics*, **2**(4), 1968, 192-197.
- [15] Johnson, V.E., Jr., *Theoretical determination of low-drag supercavitating hydrofoils and their two-dimensional characteristics at zero cavitation number*, NACA, 1957.
- [16] Johnson, V.E., Jr., The influence of depth of submergence, aspect ratio, and thickness on supercavitating hydrofoils operating at zero cavitation number, In the *Second Symposium on Naval Hydrodynamics*, ONR, Washington, U.S.A., 1958.
- [17] Kerwin, J.E., Marine propellers, *Annual Review of Fluid Mechanics*, **18**, 1986, 367-403.
- [18] Kinnas, S.A., Super-cavitating hydrofoils and propellers: Prediction of performance and design. *RTO AVT/VKI Special Course – Supercavitating Flows*, von Karmen Institute for Fluid Dynamics, 2001.
- [19] Kinnas, S.A. & Fine, N.E., Non-linear analysis of the flow around partially or super-cavitating hydrofoils by a potential based panel method. In *Boundary Integral Methods – Theory and Applications (Symposium papers)*, Springer-Verlag, 1991, 289-300.
- [20] Laberteaux, K.R. & Ceccio, S.L., Partial cavity flows: Part 1 - Cavities forming on models without spanwise variation, *Journal of Fluid Mechanics*, **431**, 2001, 1- 41.
- [21] Lamb, H., *Hydrodynamics*, Cambridge University Press, 1932.
- [22] Lang, T.G. & Daybell, D.A., "Water tunnel tests of three vented hydrofoils in two-dimensional flow, *Journal of Ship Research*, **5**(3), 1961, 1-15.
- [23] Lee, C.-S., Kim, Y.-G. et al., "A potential-based method for the analysis of a two-dimensional super- or partially-cavitating hydrofoil, *Journal of Ship Research*, **36**(2), 1992, 168-181.
- [24] Meijer, M.C., Pressure measurements on flapped hydrofoils in cavity flows and wake flows, *Journal of Ship Research*, **11**(3), 1967, 170-189.
- [25] Milne-Thomson, L.M., *Theoretical Hydrodynamics*, Dover Publications, Inc., New York, 1968.
- [26] Mishima, S. & Kinnas, S.A., A numerical optimization technique applied to the design of two-dimensional cavitating hydrofoil sections, *Journal of Ship Research*, **40**(1), 1996, 28-38.
- [27] Oba, R. & Matsudaira, Y., Effects of surface tension on supercavitating foil performance, *Institute of High Speed Mechanics*, Tohoku University, Report 268, 1974.
- [28] Parkin, B.R., Experiments on circular-arc and flat plate hydrofoils in noncavitating and full-cavity flows, California Institute of Technology Report 47-6, 1956. (See also – J. Ship Res. 1: 34-56, 1958).
- [29] Rutgersson, O., *Supercavitating propeller performance*, Swedish Maritime Research Centre, Göteborg, Sweden, SSPA Publication No. 82, 1979.
- [30] Tulin, M.P., Supercavitating flows - Small perturbation theory, *Journal of Ship Research*, **7**(3), 1964, 16-37.
- [31] Tulin, M.P. & Burkart, M.P., *Linearized theory for flows about lifting foils at zero cavitation number*, DTMB Technical Report C-638, 1955.
- [32] Watanabe, S., Tsujimoto, Y, et al., Theoretical analysis of transitional and partial cavity instabilities, *Journal of Fluids Engineering*, **123**(3), 2001, 692-69.
- [33] Wu, T.Y.-T., A free streamline theory for two-dimensional fully cavitating hydrofoils, *Journal of Mathematics and Physics*, **35**, 1956, 236-265.